Electronic Supplementary Material (ESI) for Sustainable Energy & Fuels.

Electronic Supporting Information (ESI)

Fractal growth of fern-like nanostructured Cu_2O film electrode for electrochemical reduction of CO_2 to ethanol

Deep Lata Singh,[a] Ramasamy Shanmugam,[b] Vineet Mishra,[a] and G. Ranga Rao[a]*

[a] *Department of Chemistry and DST Solar Energy Harnessing Centre (DSEHC), Indian Institute of Technology Madras, Chennai-600036, India*

[b]*Computational Insights and Sustainable Research Laboratory (CISRL), CO_2 Research and Green Technologies Centre, Vellore Institute of Technology, Vellore-632014, India*

*Corresponding Author Email: grrao@iitm.ac.in

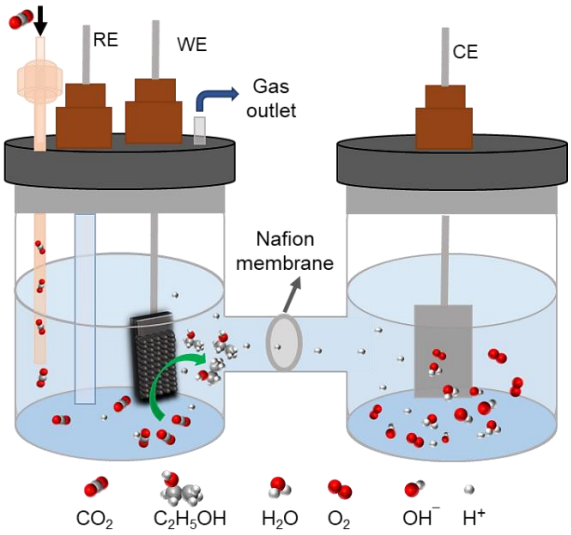

Scheme S1. Schematic diagram of the electrochemical setup (H-cell) used to carry out electrochemical CO_2 reduction.

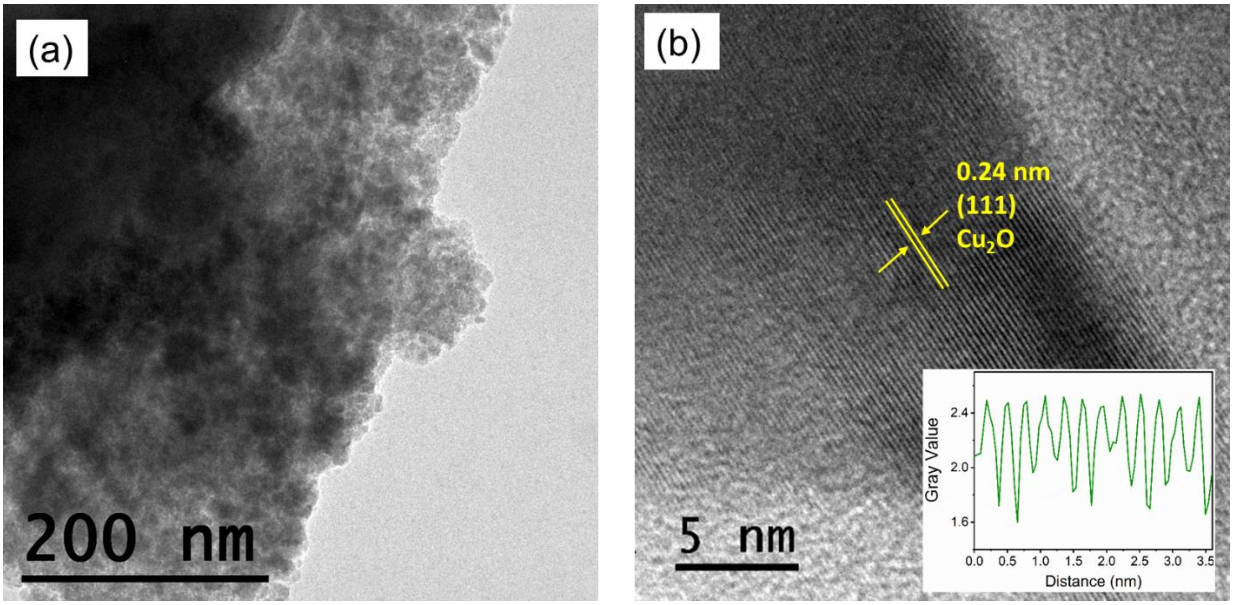

Figure S1. HR-TEM images of CuP3T5 at different magnifications.

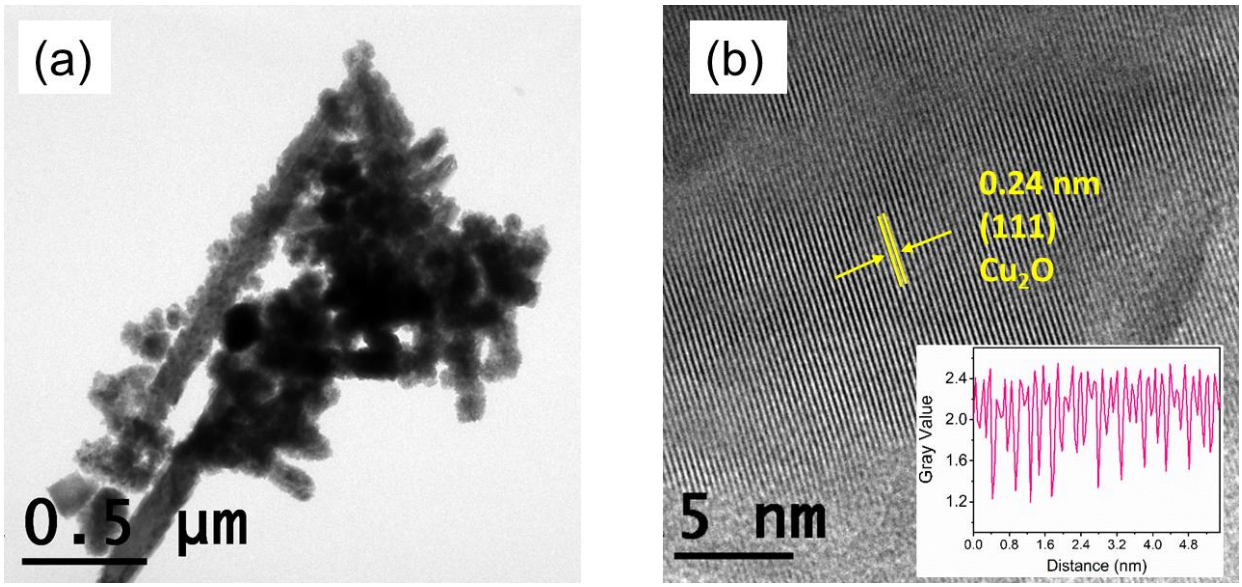

Figure S2. HR-TEM images of CuP5T5 at different magnifications.

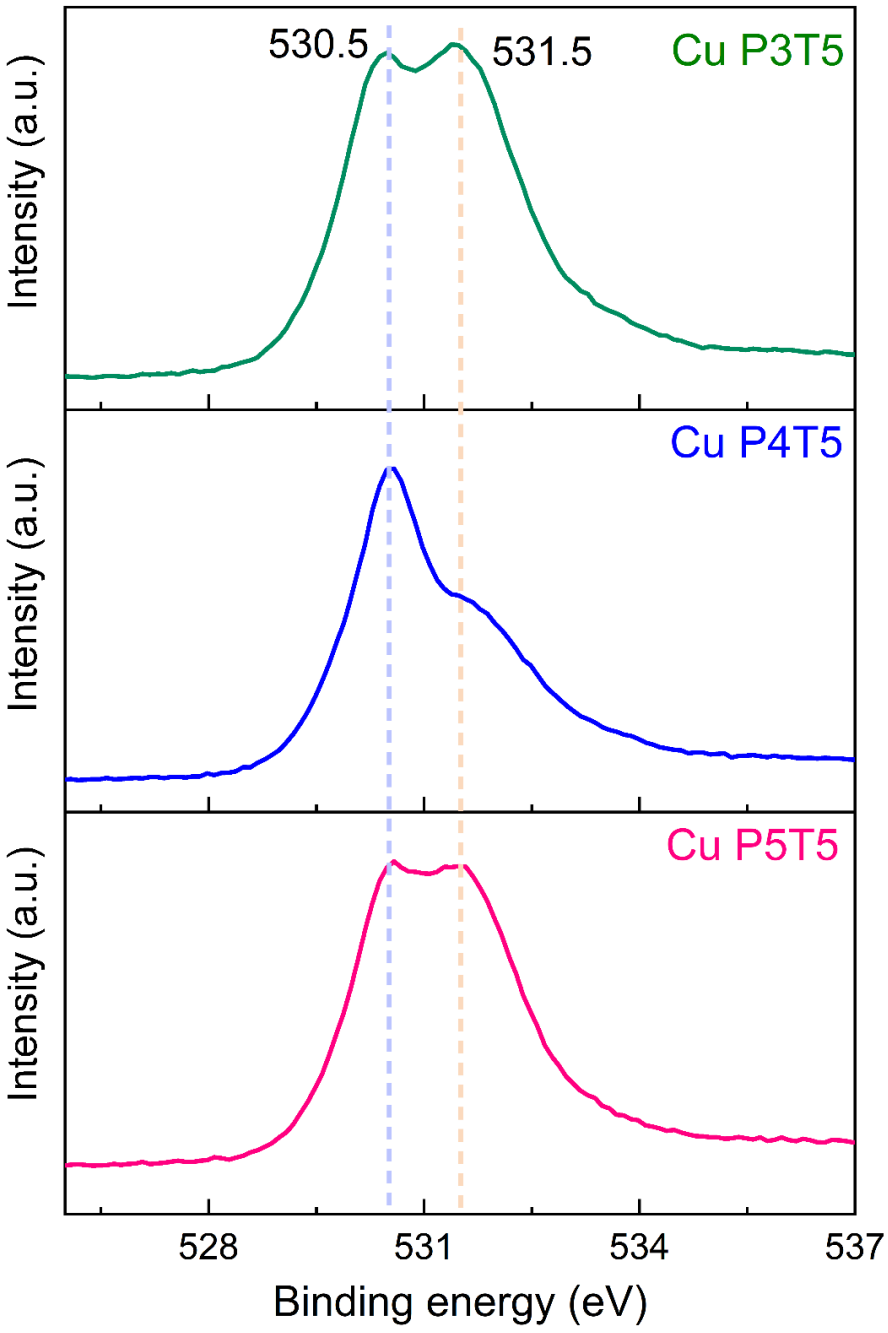

Figure S3. Core level O 1s XPS spectra of CuP3T5, CuP4T5 and CuP5T5 electrodes.

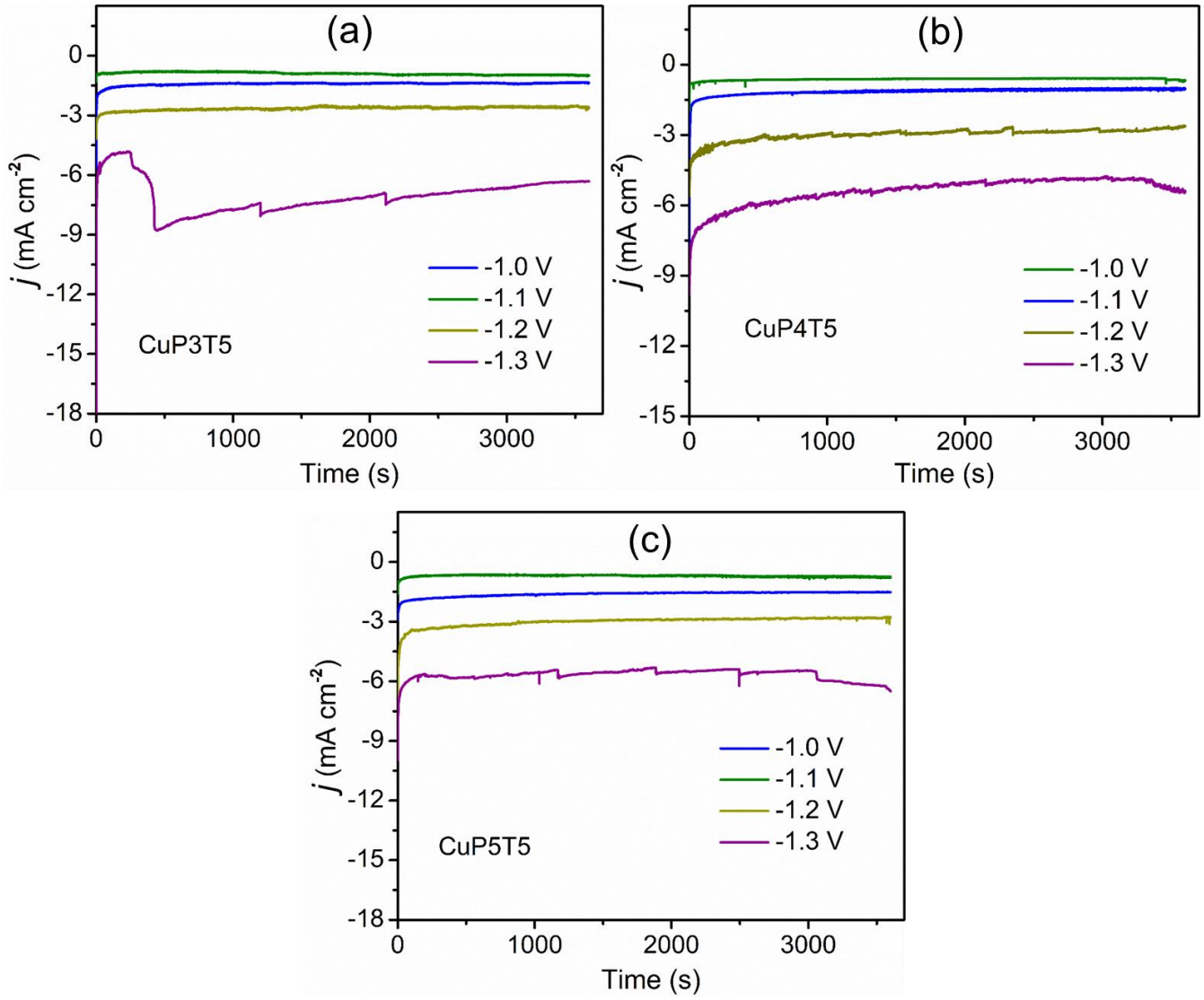

Figure S4. Chronoamperometry performances of CuP3T5, CuP4T5 and CuP5T5 film electrodes at the various applied potenial of -1.0 to -1.3 V for 1 hour in CO_2 saturated 0.1 M $KHCO_3$ electrolyte.

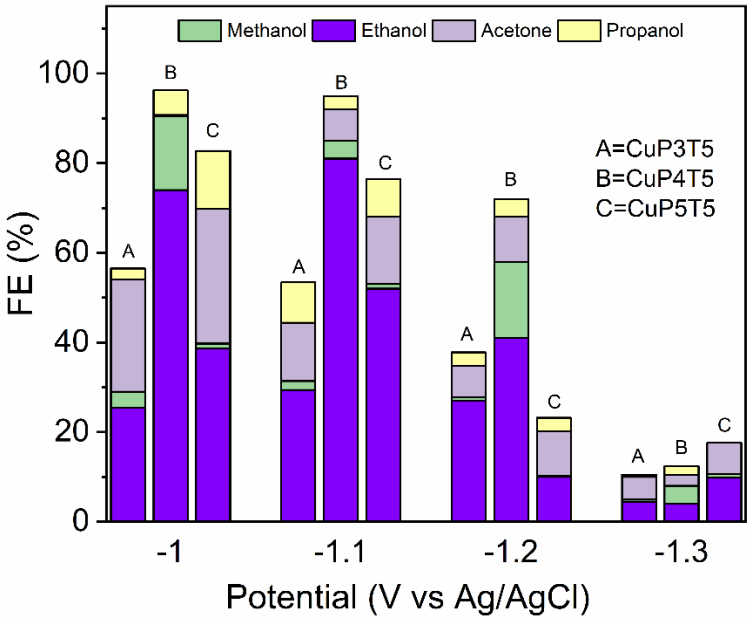

Figure S5. Faradaic efficiecies given by of CuP3T5, CuP4T5 and CuP5T5 film electrodes at the various applied potenials of -1.0 to -1.3 V in CO_2 saturated 0.1 M $KHCO_3$ electrolyte.

Table S1. Faradaic efficiecies obtained by applying 1h chronoamperometry.

Electro-deposited Materials	Potential V vs Ag/AgCl	Faradaic Efficiencies (%)			
		Ethanol	Methanol	Acetone	propanol
CuP3T5	-1.0	25.5	3.5	25	2.5
	-1.1	29.4	2	13	9
	-1.2	27	0.8	7	3
	-1.3	4.5	0.5	5	0.5
CuP4T5	-1.0	74	16.5	0.23	5.5
	-1.1	80	4	7	3
	-1.2	41	17	10	4
	-1.3	4	4	2.4	2
CuP5T5	-1.0	38.6	1.15	30	13
	-1.1	51	1	15	8.5
	-1.2	10	0.2	10	3
	-1.3	9.8	0.8	7	0

Calculation of the Faradaic efficiency:

$$FE = \frac{n \times F \times C_i \times V_i}{j \times A \times t} \times 100$$

where, n is the number of electrons, F is the Faraday constant (96485, C/mol), C_i is the concentration of the product in mol/L, V_i is volume of the catholyte in L, j=total current density in A/cm^2, A= area of the electrode in cm^2 and t is time in seconds.

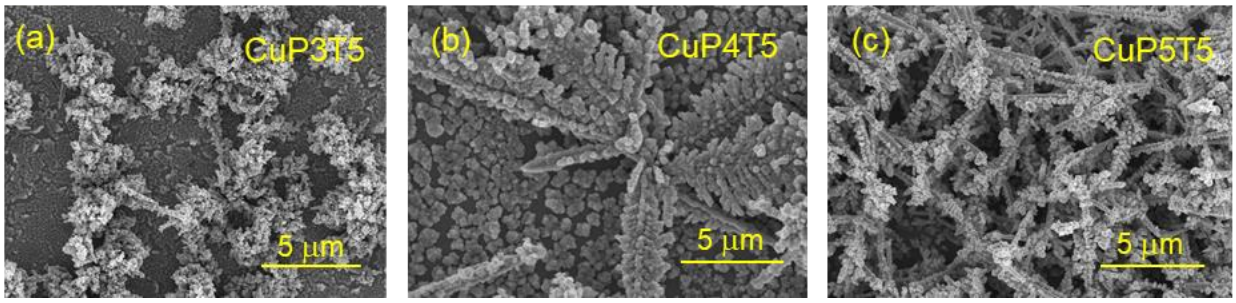

Figure S6. HR-SEM images of the film electrodes recorded after the electrochemical studies.

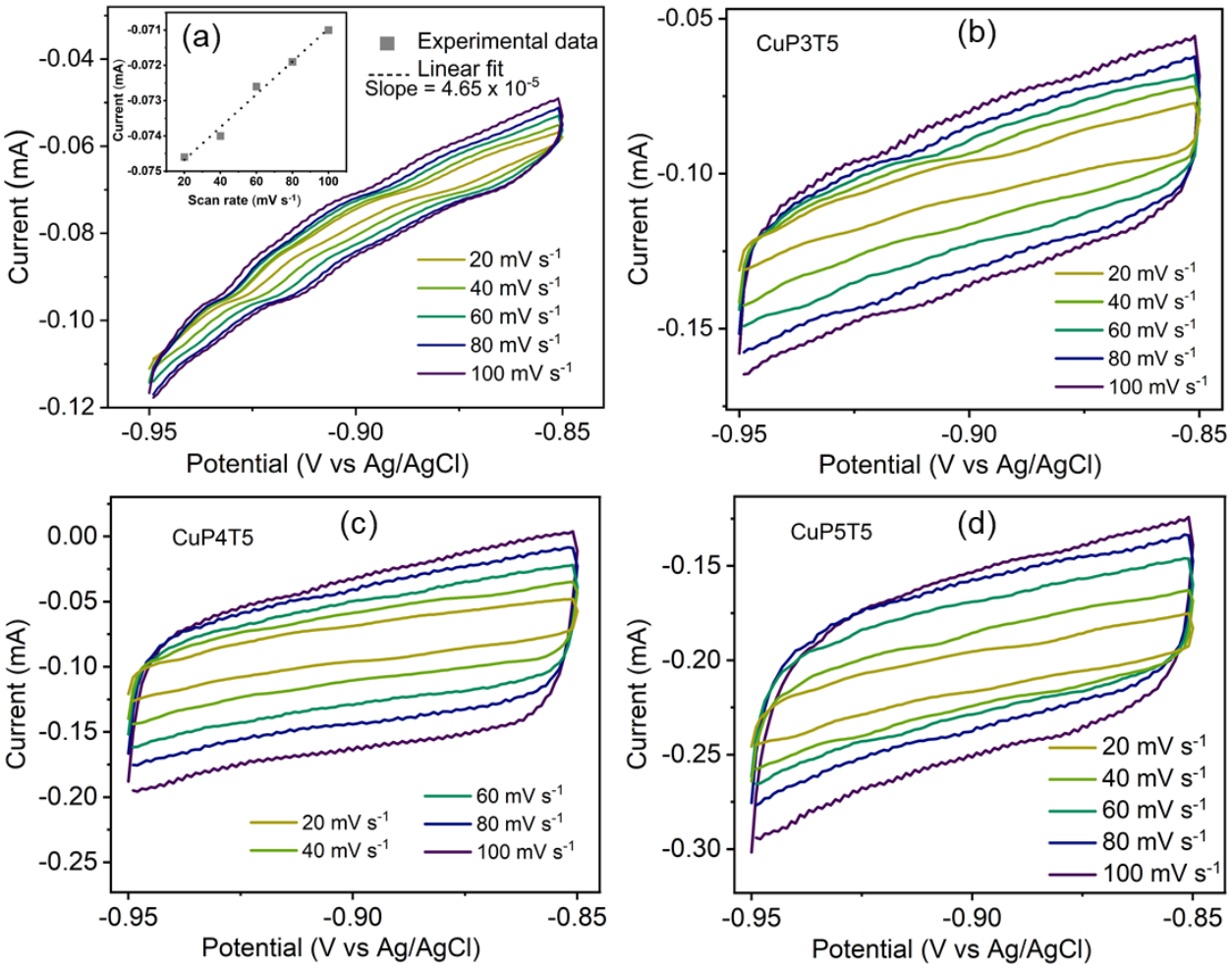

Figure S7. CV curves in the non-faradaic region at different scan rates of 20, 40, 60, 80 and 100 mV s^{-1} for (a) bare SS-316 with fitted graph, (b) CuP3T5, (c) CuP4T5 and (d) CuP5T5 film electrodes in 0.1 M $KHCO_3$ electrolyte.

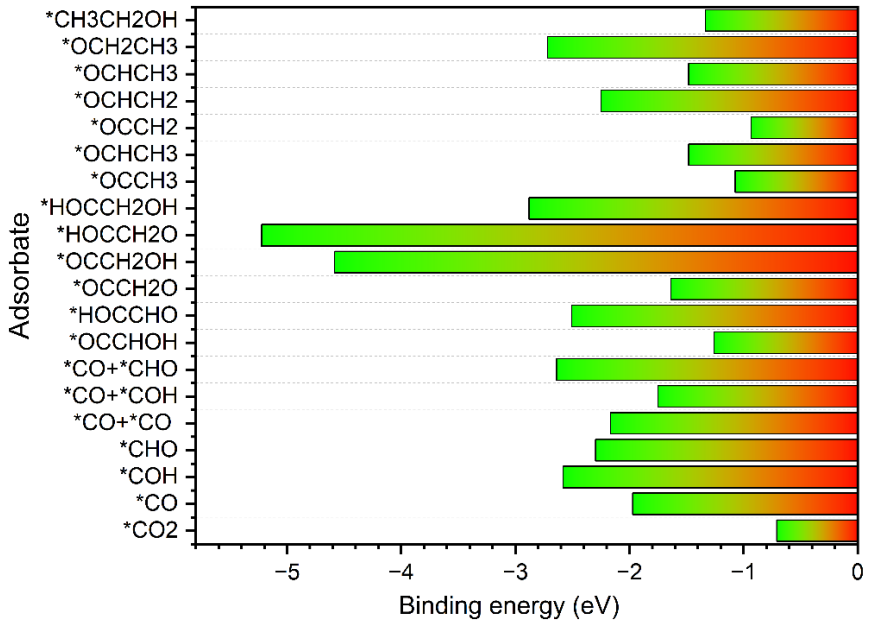

Figure S8. The adsorption binding energy of the intermediates on the surface of $Cu_2O(111)$.

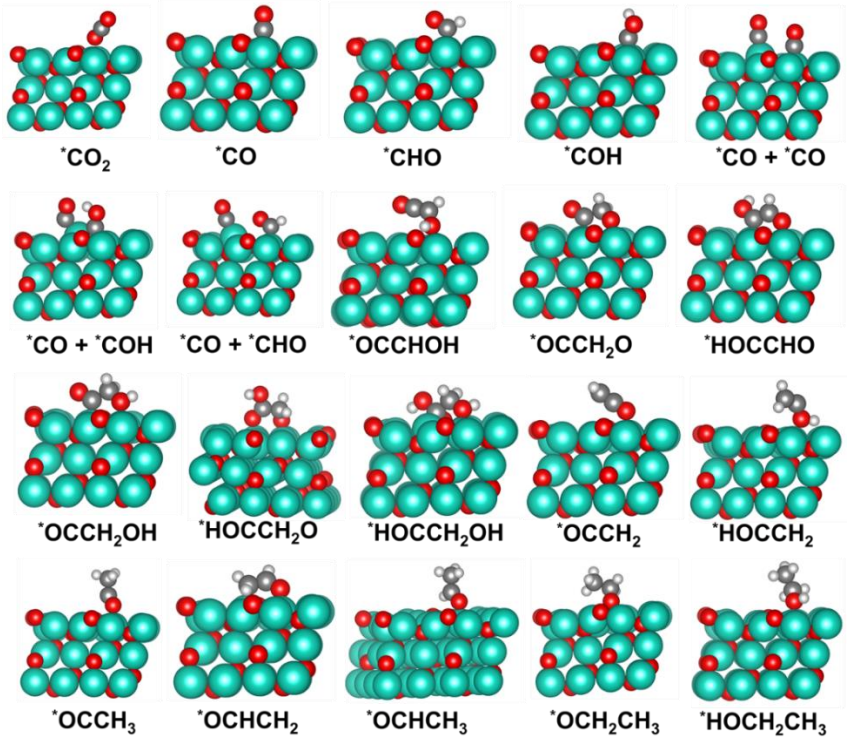

Figure S9. The energy-minimized structures that represent the different intermediates involved in the conversion of CO_2 to C_2H_5OH. The atoms are represented by the color codes Cu-cyan, O-red, C-grey, and H-white. Note: *adsorbed intermediate.

Table S2. An overview of faradaic efficiencies reported using Cu_2O based catalysts in electrochemical CO_2 reduction.

Preparation method	Sample	Substrate	Electrolyte	Product, FE (%)	E vs RHE or (Ag/AgCl)	Ref.
Galvanostatic deposition	Cu_2O	Cu disc	0.1 M $KHCO_3$	C_2H_4, 40 C_2H_5OH, 16	-0.99	[1]
Electrodeposition	Cu_2O inverse opals	FTO film	0.1 M $KHCO_3$	CO, 45.3 HCOOH, 34.5	-0.6 -0.8	[2]
Wet chemical reduction method	Cu_2O nanoparticles (NPs)	Glassy carbon electrode	0.5 M $KHCO_3$	C_2H_4, 59	-1.1	[3]
Electro-redeposition	$Cu_2(OH)_3Cl$ sol-gel	Carbon paper	0.1 M $KHCO_3$	C_2H_4, 38.5 CH_4, 0.03	-1.2	[4]
Electrodeposition	Cu_2O-derived Cu NPs	Cu plate	0.1 M $KHCO_3$	C_2H_4, 33.5 CH_4, 4.0	-1.1	[5]
Electrodeposition	Mesoporous Cu_2O	Cu foam	0.5 M $NaHCO_3$	C_2H_4, 37	-0.7	[6]
One-pot wet-chemical	Cu_2O NPs/C	Glassy carbon electrode	0.1 M $KHCO_3$	C_2H_4, 57.3	-1.1	[7]
Precipitation	multihollow Cu_2O	Hydrophobic carbon paper	2 M KOH	C_2H_4, 38 CH_3COOH, 4.8 C_2H_5OH, 26.9 C_3H_7OH, 5.5	-0.61	[8]
Template-assisted hydrothermal synthesis process.	Cu_2O-octhedral	Carbon paper	0.5 M $KHCO_3$	CH_3OH, 4.9 C_2H_5OH, 17.9 C_3H_8O, 12.6	-0.3	[9]
In-situ etching methods	Cu_2O@Cu-MOF	Glassy carbon electrode	0.1 M $KHCO_3$	CO, 1.8 CH_4, 63.2 C_2H_4, 16.2 HCOOH, 3.8 C_2H_5OH, 4.1	-1.71	[10]
Ion-track technology	Cu nanowire networks	Cu back electrode in touched with Cu plate	0.1 M $KHCO_3$	CH_4, ~0.3 C_2H_4, ~5 C_2H_6, ~2 C_2H_5OH, ~1.5 C_3H_7OH, ~3 C_2H_6O2, ~4 CH_3COOH, ~0.3	-0.83	[11]
Combined Phase inversion/ sintering	Cu_2O over Cu hollow fiber	Copper tube	0.5 M $KHCO_3$	HCOOH, 92.3	-1.18	[12]
In-situ reconstructions	Cu/Cu_2O nanoclusters	--	0.1 M $KHCO_3$	C_2H_4, 70.2	-1.03	[13]
Wet chemical method	Cu/Cu_2O nanocrystal	Hydophobic carbon paper	0.1 M K_2SO_4	C_2H_4, 38 C_2H_5OH, 30	-2.0 vs Ag/AgCl	[14]
Electrodeposition	Cu_2O (CuP4T5)	Stainless steel-316	0.1 M $KHCO_3$	C_2H_5OH, ~80 CH_3OH, ~4 Acetone, ~7 Propanol, ~3	-1.1 vs Ag/AgCl	This work

References:

1 D. Ren, Y. Deng, A. D. Handoko, C. S. Chen, S. Malkhandi and B. S. Yeo, *ACS Catal*., 2015, **5**, 2814–2821.
2 X. Zheng, J. Han, Y. Fu, Y. Deng, Y. Liu, Y. Yang, T. Wang and L. Zhang, *Nano Energy*, 2018, **48**, 93–100.
3 Y. Gao, Q. Wu, X. Liang, Z. Wang, Z. Zheng, P. Wang, Y. Liu, Y. Dai, M. H. Whangbo and B. Huang, *Adv. Sci*., 2020, **7**, 1902820.
4 P. De Luna, R. Quintero-Bermudez, C. T. Dinh, M. B. Ross, O. S. Bushuyev, P. Todorović, T. Regier, S. O. Kelley, P. Yang and E. H. Sargent, *Nat. Catal*., 2018, **1**, 103–110.
5 R. Kas, R. Kortlever, A. Milbrat, M. T. M. Koper, G. Mul, J. Baltrusaitis, *Phys. Chem. Chem. Phys*., 2014, **16**, 12194–12201.
6 A. Dutta, M. Rahaman, N. C. Luedi, M. Mohos and P. Broekmann, *ACS Catal*., 2016, **6**, 3804–3814.
7 H. Jung, S. Y. Lee, C. W. Lee, M. K. Cho, D. H. Won, C. Kim, H. S. Oh, B. K. Min and Y. J. Hwang, *J. Am. Chem. Soc*., 2019, **141**, 4624–4633.
8 P. P. Yang, X. L. Zhang, F. Y. Gao, Y. R. Zheng, Z. Z. Niu, X. Yu, R. Liu, Z. Z. Wu, S. Qin, L. P. Chi, Y. Duan, T. Ma, X. S. Zheng, J. F. Zhu, H. J. Wang, M. R. Gao and S. H. Yu, *J. Am. Chem. Soc*., 2020, **142**, 6400–6408.
9 B. Liu, X. Yao, Z. Zhang, C. Li, J. Zhang, P. Wang, J. Zhao, Y. Guo, J. Sun and C. Zhao, *ACS Appl. Mater. Interfaces*, 2021, **13**, 39165–39177.
10 X. Tan, C. Yu, C. Zhao, H. Huang, X. Yao, X. Han, W. Guo, S. Cui, H. Huang and J. Qiu, *ACS Appl. Mater. Interfaces*, 2019, **11**, 9904−9910.
11 N. Ulrich, M. Schäfer, M. Römer, S. D. Straub, S. Zhang, J. Brötz, C. Trautmann, C. Scheu, B. J. M. Etzold and M. E. Toimil-Molares. *ACS Appl. Nano Mater*., 2023, **6**, 4190–4200.
12 G. Li, Y. Song, C. Zhu, X. Dong, W. Chen, G. Wu, G. Feng, S. Li and W. Wei, *J. CO_2 Util*., 2023, **70**, 102446.
13 C. Liu, X. D. Zhang, J. M. Huang, M. X. Guan, M. Xu and Z. Y. Gu, *ACS Catal*., 2022, **12**, 15230–15240.
14 Y. Yang, Z. Tan, S. Wang, Y. Wang, J. Hu, Z. Su, Y. Zhao, J. Tai and J. Zhang, *Chem. Commun*., 2023, **59**, 2445–2448.